An Introduction to the Dimer Model

Richard Kenyon*

Laboratoire de Mathématiques, Université Paris-Sud, Orsay, France

Lectures given at the
School and Conference on Probability Theory
Trieste, 13-31 May 2002

LNS0417005

*Richard.Kenyon@math.u-psud.fr

Contents

1 Introduction

A **perfect matching** of a graph is a subset of edges which covers every vertex exactly once, that is, for every vertex there is exactly one edge in the set with that vertex as endpoint. The **dimer model** is the study of the set of perfect matchings of a (possibly infinite) graph. The most well-known example is when the graph is $\mathbb{Z}^2$, for which perfect matchings are equivalent (via a simple duality) to **domino tilings**, that is, tilings of the plane with 2×1 and 1×2 rectangles.

In the first three sections we study domino tilings of the plane and of finite polygonal regions, or equivalently, perfect matchings on $\mathbb{Z}^2$ and subgraphs of $\mathbb{Z}^2$.

In the last two sections we study the FK-percolation model and the dimer model on a more general family of planar graphs.

2 The number of domino tilings of a chessboard

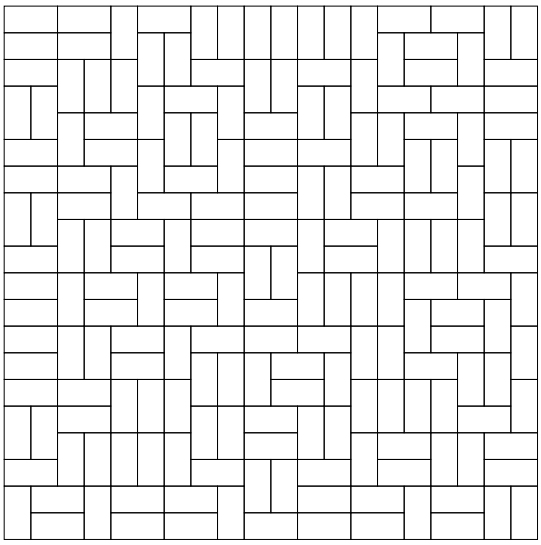

Figure 1: Random tiling of a square

A famous result of Kasteleyn [8] and Temperley and Fisher [18] counts the number of domino tilings of a chessboard (or any other rectangular region).

In this section we explain Kasteleyn's proof.

2.1 Combinatorics

Let R be the region bounded by a simple closed polygonal curve in $\mathbb{Z}^2$. A domino tiling of R corresponds to a perfect matching of G, the dual graph of R: G has a vertex for each lattice square in R, with two vertices adjacent if and only if the corresponding lattice squares share an edge.

Theorem 1 *[Kasteleyn, 1961] The number of domino tilings of R is $\sqrt{|\det K|}$, where K is the weighted adjacency matrix of the graph G, with horizontal edges weighted 1 and vertical edges weighted $i = \sqrt{-1}$.*

For example for the 2×3 region in Figure 2, the matrix K is

$$K = \begin{pmatrix} 0 & 0 & 0 & i & 1 & 0 \\ 0 & 0 & 0 & 1 & i & 1 \\ 0 & 0 & 0 & 0 & 1 & i \\ i & 1 & 0 & 0 & 0 & 0 \\ 1 & i & 1 & 0 & 0 & 0 \\ 0 & 1 & i & 0 & 0 & 0 \end{pmatrix},$$

whose determinant has absolute value $9 = 3^2$.

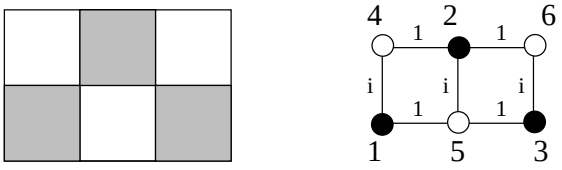

Figure 2: 2×3 rectangle and dual graph.

Proof: Since the graph G is bipartite (one can color vertices black and white so that black vertices are only adjacent to white vertices and vice versa) K can be written $K = \begin{pmatrix} 0 & A \\ A^t & 0 \end{pmatrix}$, so we must evaluate

$$\det A = \sum_{\sigma \in S_n} \mathrm{sgn}\sigma k_{1\sigma(1)} \dots k_{n\sigma(n)}$$

Each term in this sum is zero unless black vertex $\sigma(i)$ is adjacent to white vertex i for each i. Therefore we have exactly one term for each matching of G. It suffices to show that two nonzero terms have the same sign.

Suppose we have two matchings; draw them one on top of the other. Their superposition is a union of (doubled) edges and disjoint cycles. One can transform the first matching into the second by "rotating" each cycle in turn. In particular it suffices to show that if two matchings differ only along a single cycle, the corresponding terms in the determinant have the same sign.

This is supplied by the following lemma, which is easily proved by induction. □

Lemma 1 *Let $C = \{v_0, \ldots, v_{2k-1}, v_{2k} = v_0\}$ be a simple closed curve in $\mathbb{Z}^2$. Let m_1 be the product of the weights on edges $v_0v_1, v_2v_3, \ldots$ and m_2 the product of the weights on the remaining edges $v_1v_2, \ldots$ (recall that vertical edges are weighted i and horizontal edges 1). Then $m_1 = (-1)^{n+k+1}m_2$, where n is the number of vertices strictly enclosed by c and k is $1/2$ of the length of c.*

2.2 Rectangles

Suppose the graph G is an m by n rectangle, with vertices $\{1, 2, \ldots, m\} \times \{1, 2, \ldots, n\}$. To compute the determinant of its adjacency matrix, we compute its eigenvectors and their eigenvalues.

For $j, k \in \mathbb{Z}$ define

$$f(x, y) = \sin \frac{\pi jx}{m+1} \sin \frac{\pi ky}{n+1}.$$

It is easy to check that f is an eigenvector of K, with eigenvalue

$$2 \cos \frac{\pi j}{m+1} + 2i \cos \frac{\pi k}{n+1}.$$

We didn't pull this formula out of a hat: since G is a "product" of two line graphs, the eigenvectors are the product of the eigenvectors of the line graphs individually.

As j, k vary over integers in $[1, m] \times [1, n]$, the f form an orthogonal basis of eigenvectors. Therefore the determinant of K is

$$\det K = \prod_{j=1}^{m} \prod_{k=1}^{n} 2 \cos \frac{\pi j}{m+1} + 2i \cos \frac{\pi k}{n+1}.$$

Evaluating $\sqrt{|\det K|}$ for $m = n = 8$ gives 12988816 tilings of a chessboard.

One may show that for m, n both large the number of tilings is $\exp(Gmn/\pi + O(m+n))$, where $G = 1 - \frac{1}{3^2} + \frac{1}{5^2} - \frac{1}{7^2} + \dots$ is Catalan's constant.

2.3 Tori

It will be useful shortly to compute the number of tilings for a graph on a torus as well (e.g. a rectangle with its opposite sides identified). Kasteleyn showed that this could be accomplished by a linear combination of four determinants. In essence these four determinants correspond to the four inequivalent "discrete spin structures" on the graph G embedded on the torus. Rather than go into details, we just note that the above proof fails on a torus since two matchings may differ on a loop which goes around the torus (is not null-homologous). The change in sign in the determinant from one matching to the next is then a function of the homology class in $H_1(\mathbb{T}, \mathbb{Z}/2\mathbb{Z})$ of the loop. The result is that (for m, n both even) the number of tilings of an $m \times n$ torus is

$$Z_{m,n} = \frac{1}{2}(-P_{00} + P_{01} + P_{10} + P_{11}),$$

where

$$P_{\sigma\tau} = \prod_{z^m=(-1)^\sigma} \prod_{w^n=(-1)^\tau} \left(z + \frac{1}{z} + iw + \frac{i}{w} \right).$$

Note that actually $P_{00} = 0$ in this case. For details see [8] or [4].

One can show that

$$\lim_{m,n\to\infty} \frac{1}{mn} \log Z_{m,n} = \frac{G}{\pi}.$$

2.4 Inverse Kasteleyn matrix

We are primarily interested in the **uniform measure** on perfect matchings of a graph G.

A very useful consequence of Kasteleyn's counting theorem is

Theorem 2 ([10]) *Let $T = \{(w_1, b_1), \dots, (w_k, b_k)\}$ be a subset of dimers, (with the jth dimer covering white vertex w_j and black vertex b_j). The probability that all dimers in T appear in a uniformly chosen matching is*

$$\Pr(T) = |\det(K^{-1}(w_i, b_j))_{1\le i,j\le k}|.$$

The advantage of this result is that the determinant for the joint probability of k dimers is of size k *independently of the size of the matrix* K. In particular to compute the probability that a single edge appears, one just needs a single element of K^{-1}.

If we can compute asymptotics of K^{-1} for large rectangles we can then understand easily the limiting measures on tilings of the plane. We'll do this later.

A more general class of measures on perfect matchings uses graphs with weighted edges. If edges are weighted $\nu(e) > 0$, the weight of a perfect matching is the product of its edge weights, and the probability measure we are interested in is that which gives a matching a probability proportional to its weight (for finite graphs). There is a simple generalization of Theorems 1 and 2 for weighted graphs.

We should also point out that versions of Theorems 1 and 2 hold for arbitrary planar graphs, see [9] and [10].

3 The arctic circle phenomenon

The order-n Aztec diamond is the region shown. It was defined and studied in [6, 3]. A random tiling is also shown. Why does it not look homogeneous, as does the tiling of a square?

Near the corners, you only see tiles of one "type". The way to understand this phenomenon is via the height function.

3.1 Heights

A domino tiling can be thought of as an interface in $2 + 1$ dimensions. Specifically, to a tiling we associate an integer-valued function h on the vertices of the region tiled, as follows. Rather than define the height, we define the height difference between two adjacent lattice points. If edge vw is not crossed by a domino, the height difference $h(w) - h(v)$ is 1 if the face to the left of vw is black, and -1 otherwise. If the edge is crossed by a domino, $h(w) - h(v)$ is -3 or $+3$ according to whether the face to the left is black or white. This defines a "one-form", that is a function on the oriented edges of the graph G satisfying $f(-e) = -f(e)$. Moreover the one-form is closed: the sum around any oriented cycle is zero (since the sum around any face is zero: a domino crosses exactly one edge of each face). Therefore

there is a function h, well defined up to an additive constant, with these edge-differences.

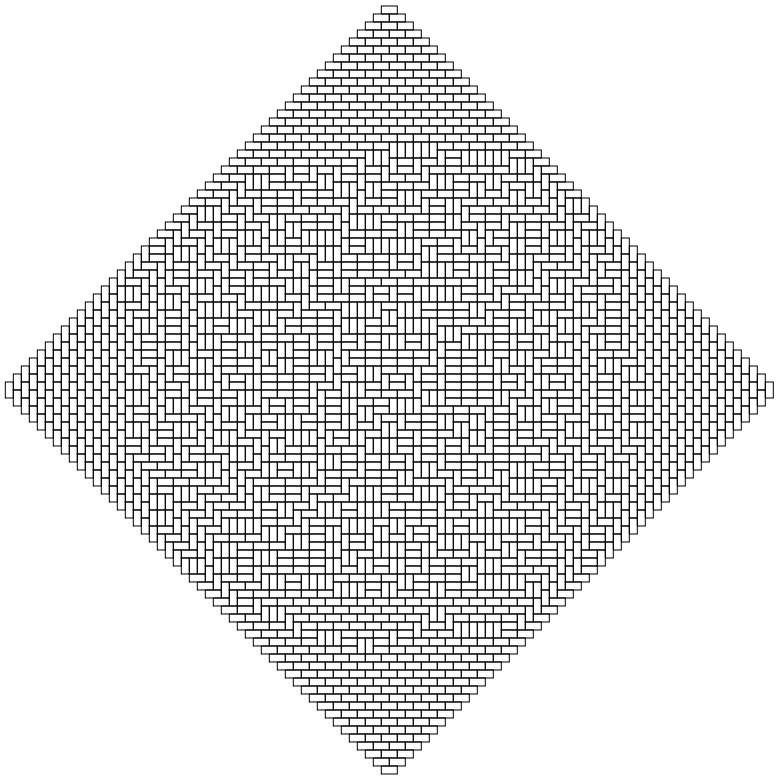

Figure 3: Random tiling of Aztec diamond

The height function of a tiling gives a map from $\mathbb{Z}^2$ to $\mathbb{Z}$. One of the principal motivations for studying dominos is to study the model of random maps of this sort.

Note that a tiling determines a height function, and vice versa. Also, the height function on the boundary of the region to be tiled is independent of the tiling.

For the $2n \times 2n$ square, the boundary function is asymptotically flat, in fact assuming the value at a corner is 0, it alternates on edge edge between 0 and 1 or 0 and -1: see Figure 4. However for the Aztec diamond of order n, it is linear on each edge:

For a non-planar region such as a torus, the height might not be well-defined: it can be well-defined locally, but on a path winding around the

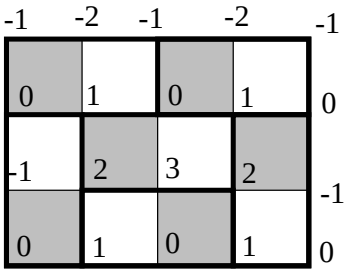

Figure 4: Heights in a domino tiling.

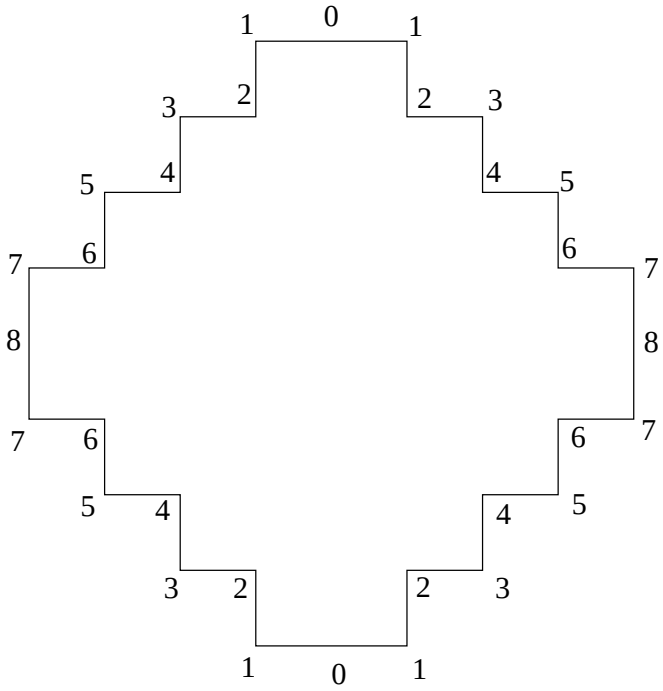

Figure 5: Heights on boundary of an Aztec diamond.

torus it may have a non-trivial period. Indeed, for a graph on the $m \times n$ torus the height will have a well-defined horizontal period h_x and vertical period h_y, both integers, such that the height change on any closed path winding once horizontally around the torus is h_x, and similary h_y for vertically-winding paths.

The height of a random tiling on a planar region is a random function with those given boundary values. It is easy to guess that the height at an interior point of a random tiling of a square of side n is $o(n)$. However for the Aztec diamond it is not at all clear what the height of a random tiling will be. In fact it will typically lie near (within $o(n)$) of its mean value. Moreover its mean value can be determined by solving a certain variational principle (minimizing a certain energy). That is the content of this section.

3.2 CKP theorem

The theorem of Cohn-Kenyon-Propp states this in general: given a Jordan domain U with function $u : \partial U \to \mathbb{R}$, and a sequence of domains in $\epsilon\mathbb{Z}^2$ converging to U, with boundary height functions h_ϵ converging to u, that is $\epsilon h_\epsilon \to u$, then with probability tending to 1 the height of a random tiling will lie near (within $o(n)$) its mean value, and the mean value h_0 is the unique function f maximizing a certain "entropy"

$$\mathrm{Ent}(f) = \int_U \mathrm{ent}(\partial_x f, \partial_y f) dx dy.$$

Here

$$\mathrm{ent}(s,t) = \frac{1}{\pi}\left(L(\pi p_a) + L(\pi p_b) + L(\pi p_c) + L(\pi p_d)\right),$$

where $L(x) = -\int_0^x \log 2 \sin t dt$ is Lobachevsky's function, and p_a, p_b, p_c, p_d are certain probabilities which are determined by the following equations.

$$\begin{aligned} 2(p_a - p_b) &= s \\ 2(p_d - p_c) &= t \\ p_a + p_b + p_c + p_d &= 1 \\ \sin \pi p_a \sin \pi p_b &= \sin \pi p_c \sin \pi p_d. \end{aligned}$$

The proof of the first part of this theorem is somewhat standard. The harder part is the computation of the function ent.

The idea of the proof of the first part is the following. Each height function is a Lipschitz function with Lipschitz constant 3, since $|f(x_1, y_1) -$

$f(x_1+1, y_1)| \leq 3$ and similarly for the y-direction. In fact we have a stronger condition that when $x_1 - x_2, y_1 - y_2$ are even,

$$|f(x_1, y_1) - f(x_2, y_2)| \leq 2 \max\{|x_1 - x_2|, |y_1 - y_2|\} \tag{1}$$

Let L be the class of functions satisfying (1). When we scale the $x-$ and y-coordinates by ϵ, then ϵf is still in L. Note that L is compact (in the uniform topology).

On this space, the functional Ent is upper semicontinuous: its value can only increase at a limit point. This follows from the strict concavity of the function $\mathrm{ent}(s,t)$. Concavity also proves unicity of the maximizing function.

Since L is compact, cover it with a finite number of metric balls $B_f(\delta)$ of radius δ. We will show that for any $f \in L$, the number of tilings for which ϵh lies within δ of f is $\exp(\frac{1}{\epsilon^2}\mathrm{Ent}(f)(1 + o(1)))$. This determines the size of each $B_f(\delta)$. Therefore when ϵ is small, the number of tilings whose normalized height function lies close to $f_{\max}$ overwhelmingly dominates the number of other tilings, even combined.

Thus almost all tilings lie near $f_{\max}$.

To count the number of tilings whose height function lies near a given function $f \in L$, triangulate U with a fine mesh, large on the scale of ϵ but with mesh size tending to zero. Since a Lipschitz function is differentiable almost everywhere, on almost all triangles the function f is almost linear. A tiling which lies close to f will lie close to a linear function on most triangles. So it suffices to count the number of tilings whose height function is close to a linear function.

However a short technical lemma (essentially subadditivity) proves that if R is a triangular region (or other nice region), the number of tilings with height function lying close to a fixed linear function ℓ on that region is $\exp(A \cdot \mathrm{ent}(\ell) \cdot (1 + o(1)))$, where A is the area of R and $\mathrm{ent}(\ell)$ is a function depending only on the slope of ℓ.

The explicit computation of $\mathrm{ent}(s,t)$ comes from computing the number of tilings on a torus with a given slope (s,t), that is, a given horizontal height change $[sm]$ going horizontally around the torus, and $[tn]$ vertically.

To compute this we use staggered weights a, b, c, d on the edges of $\mathbb{Z}^2$, as in Figure 6.

If we put these weights in the Kasteleyn matrix then its determinant is the sum over tilings of the weight of a tiling (product of the edge weights). That is, $\sqrt{|\det K|}$ is the **partition function** $Z(a,b,c,d)$ of tilings with

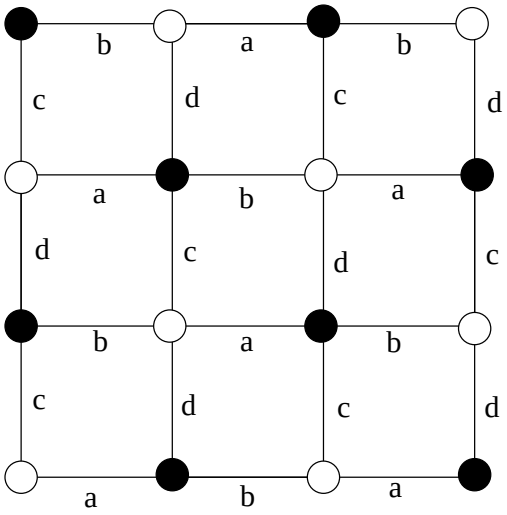

Figure 6: Weights on torus graph

these weights. For a tiling of the torus with these weights, the number of dominos of type a, b, c, d determines the height change around the torus: the horizontal height change is $(N_d - N_c)/n$ and the vertical height change is $(N_a - N_b)/m$. Therefore once we know

$$Z(a,b,c,d) = \sum_{\text{matchings}} a^{N_a} b^{N_b} c^{N_c} d^{N_d}$$

we have

$$Z(a,1/a,c,1/c) = \sum_{\text{matchings}} a^{mh_y} c^{-nh_x}$$

and we need only extract the appropriate coefficient to get the number of tilings of given slope.

In [4] the asymtotic formula is given

$$\log Z(a,b,c,d) = \frac{1}{(2\pi i)^2} \int_{S^1} \int_{S^1} \log(a + bz + cw + dzw) \frac{dz}{z} \frac{dw}{w},$$

from which the above formula for ent follows.

3.3 Flats

For the Aztec diamond, the function $f_{\max}$ is not analytic, only piecewise analytic. In the four regions outside of the inscribed circle $f_{\max}$ is linear (as you can approximately see in the example tiling). Inside it is analytic. On the boundary of the inscribed circle (the **arctic circle**, since it separates the "frozen region" from the "temperate" zone) the function is C^1 but not C^2. In fact it is $C^{1.5}$ except at the four boundary-edge midpoints.

These frozen regions result from the degeneration of the ellipticity of the PDE defining $f_{\max}$ at the boundary of the domain of definition.

It is very interesting to study what happens exactly at the boundary. We won't discuss this here though.

4 Conformal invariance

The scaling limit (limit when the lattice spacing tends to zero) of the height function on domino tilings tends to a nice conformally invariant continuous process, the "massless Gaussian free field", a sort of two-dimensional version of Brownian motion. In this section we discuss the ideas behind the proof. The original references are [11, 12].

4.1 K as Dirac operator

We had a lot of choice in definition of the Kasteleyn matrix. If you go back to the proof, you will see that we could have chosen any edge weights with the property that the weights on a lattice square $\alpha, \beta, \gamma, \delta$ satisfy the condition that $\alpha\gamma/\beta\delta$ is real and negative. It is convenient to put weights as in Figure 7.

Lemma 1 holds for these weights as well, as do Theorems 1 and 2.

Let us now study K^{-1} for these weights. Because of bipartiteness, $K^{-1}(v_1, v_2) = 0$ unless one of v_1, v_2 is black and the other is white. Let B denote the black vertices and W the white vertices. Let $w \in W$. If $f \in \mathbb{C}^B$, then $Kf \equiv 0$ means

$$f(w+1) - f(w-1) + i(f(w+i) - f(w-i)) = 0$$

that is "$\partial_x + i\partial_y$" $f = 0$. We say $f \in \mathbb{C}^B$ is **discrete analytic** if $Kf = 0$.

Let B_0, B_1 be the black vertices whose coordinates are both even (respectively, both odd). Similarly let W_0, W_1 be the white vertices whose coordinates are $(1,0)$ mod 2, respectively $(0,1)$ mod 2.

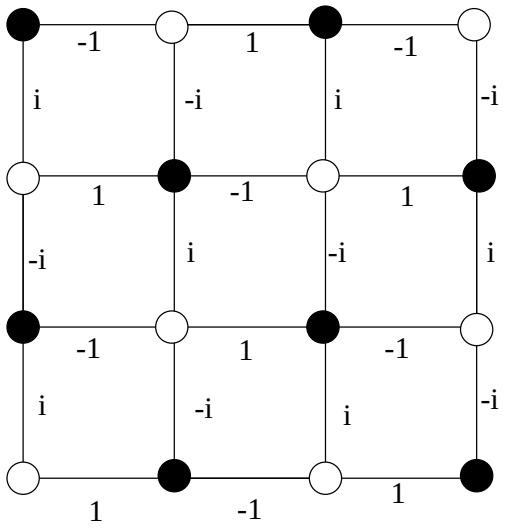

Figure 7:

Lemma 2 *If $f \in \mathbb{C}^B$ is discrete analytic, then f is harmonic on B_0 and B_1 separately, that is,*

$$4f(b) = f(b+2) + f(b-2) + f(b+2i) + f(b-2i).$$

Moreover, these two harmonic functions are conjugate.

The proof follows from the observation that K^*K is the Laplacian when restricted to any of the sublattices B_0, B_1, W_0, W_1, see Figure 8.

As a consequence K^{-1} can be related to the Green's function.

4.2 K^{-1} and the Green's function

For a fixed w, $K^{-1}(w, b)$ (considered as a function of b) is discrete analytic, except at w. This follows from $KK^{-1} = I$.

In fact K^{-1} can be written in terms of the Green's function G. Recall that $G(u, v)$ is defined to be the function satisfying $\Delta G(u, v) = \delta_u(v)$ (taking the Laplacian wrt the second variable). For a fixed w,

$$\Delta K^{-1}(w, \cdot) = K^*KK^{-1}(w, \cdot) = (K^*\delta_w)(\cdot) = \delta_{w+1} - \delta_{w-1} - i(\delta_{w+i} - \delta_{w-i}).$$

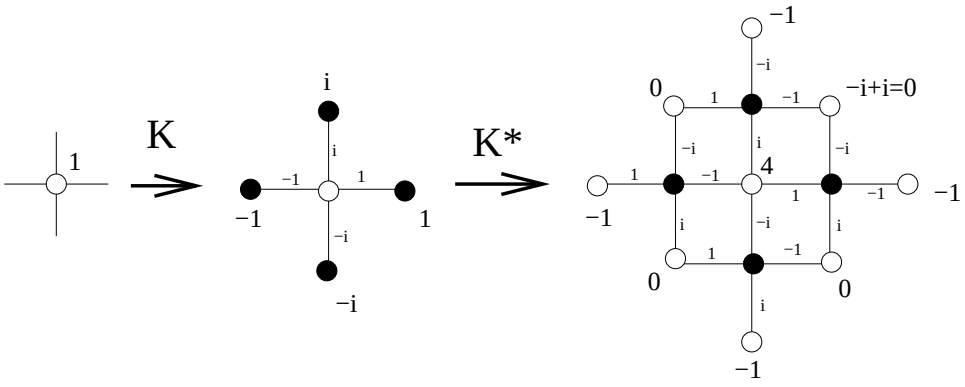

Figure 8:

Thus $K^{-1}(w,\cdot)$ is a sum of four Green's functions. When restricted to B_0, it is the difference of two Greens functions, $K^{-1}(w,b) = G(w+1,b) - G(w-1,b)$.

4.3 On a rectangle

We can easily compute K^{-1} for a rectangle, since we already diagonalized the matrix K. Because K is symmetric, we have the following:

$$K^{-1}(v_1,v_2) = \sum_j f_j(v_1) f_j(v_2)/\lambda_j$$

where f_j are the orthonormalized eigenvectors with eigenvalue λ_j.

In the limit when the rectangle gets large, and v_1, v_2 are far from the boundaries, we can find

$$K^{-1}(v_1,v_2) = \frac{1}{4\pi^2}\int_0^{2\pi}\int_0^{2\pi} \frac{e^{i(x\theta+y\phi)}}{2i\sin\theta - 2\sin\phi} d\theta d\phi, \tag{1}$$

where $(x,y) = v_2 - v_1 \in \mathbb{Z}^2$.

This formula defines, along with Theorem 2, a measure on tilings of the plane. This measure is the unique weak limit of measures on rectangles. It is also the unique entropy-maximizing translation-invariant measure on tilings [2]. Some values of K^{-1} are shown in Figure 9.

Asymptotically, if $w \in W_0$, we have

$$K^{-1}(w,b) = \begin{cases} \mathrm{Re}\frac{1}{\pi(b-w)} + O(\frac{1}{|b-w|^2}) & b \in B_0 \\ i\mathrm{Im}\frac{1}{\pi(b-w)} + O(\frac{1}{|b-w|^2}) & b \in B_1. \end{cases}$$

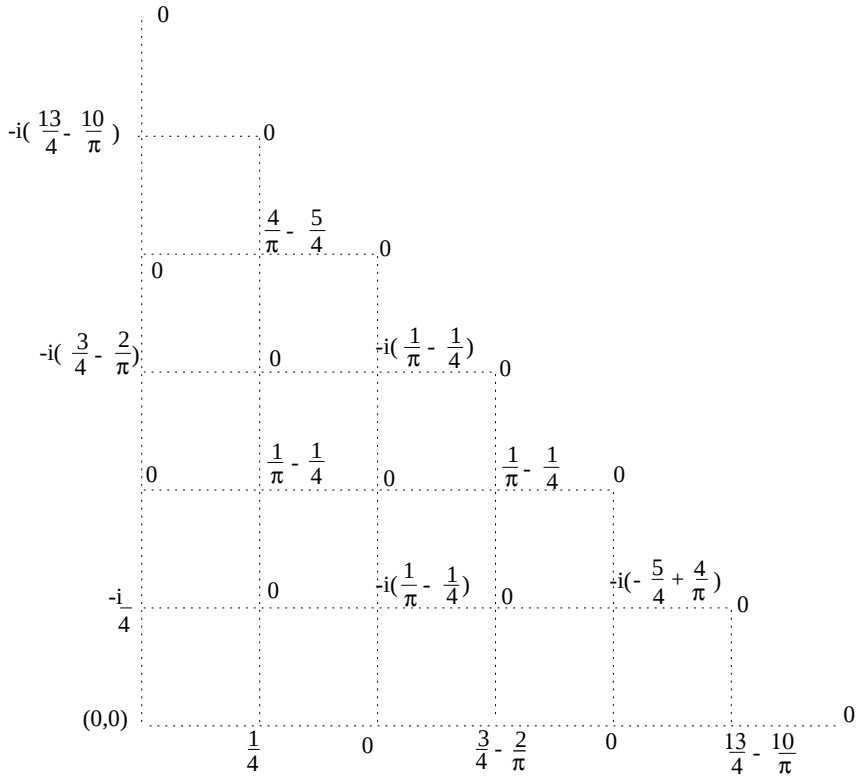

Figure 9:

These are reversed if $w \in W_1$.

4.4 Bounded domains

We can similarly compute the asymptotics of K^{-1} on bounded domains.

Let U be a Jordan domain. Let $U_{2\epsilon}$ be a domain in $2\epsilon\mathbb{Z}^2$ which approximates U. It is a well-known fact that the discrete Dirichlet Green's function on $U_{2\epsilon}$ (defined by: $G(x,y)$ is the expected number of passages at y of a simple random walk started at x and stopped at the boundary, alternatively, $G(x,y)$ is the inverse of the discrete Laplacian with Dirichlet boundary conditions) approximates the continuous Dirichlet Green's function on U.

We can use this fact to construct a graph $U_\epsilon \in \epsilon\mathbb{Z}^2$ for which the K^{-1} operator converges nicely to the corresponding continuous object on U.

The graph U_ϵ has a black vertex for each vertex and face of $U_{2\epsilon}$, and a white vertex for each edge of $U_{2\epsilon}$ (and U_ϵ is the superposition of $U_{2\epsilon}$ and its dual). However we remove from U_ϵ one black vertex b_0 on the outer face.

Lemma 3 *U_ϵ has the same number of black and white vertices.*

This follows simply from the Euler formula $V - E + F = 1$ applied to $U_{2\epsilon}$. In fact spanning trees of $U_{2\epsilon}$ rooted at b_0 are in bijection with perfect matchings of U_ϵ (see [17, 14]).

Let $G(u,v)$ be the continuous Dirichlet Green's function on U. Let $\tilde{G}(u,v)$ be the analytic function of v whose real part is $G(u,v)$. On U_ϵ we have $K^{-1} = 2\epsilon d\tilde{G} + o(\epsilon)$, in the following sense. Define F_0, F_1 and F_+, F_- by

$$\begin{aligned} d\tilde{G}(u,v) &= \frac{1}{2}(F_0(u,v)du_x + iF_1(u,v)du_y) \\ &= \frac{1}{4}(F_+(u,v)du + F_-(u,v)d\bar{u}). \end{aligned}$$

Theorem 3 *When $|w-b|$ is not $O(\epsilon)$ we have*

$$K^{-1}(w,b) = \begin{cases} \epsilon ReF_0(w,b) + o(\epsilon) & w \in W_0 \text{ and } b \in B_0 \\ \epsilon iImF_0(w,b) + o(\epsilon) & w \in W_0 \text{ and } b \in B_1 \\ \epsilon ReF_1(w,b) + o(\epsilon) & w \in W_1 \text{ and } b \in B_0 \\ \epsilon iImF_1(w,b) + o(\epsilon) & w \in W_1 \text{ and } b \in B_1. \end{cases}$$

For example on $\mathbb{R}^2$ we have $\tilde{G}(u,v) = -\frac{1}{2\pi}\log(v-u)$, so $d\tilde{G} = \frac{1}{2\pi}\frac{du_x + idu_y}{v-u}$ and $F_0 = F_1 = \frac{1}{\pi}\frac{1}{v-u}$. As another example, on the upper half plane we have $\tilde{G}(u,v) = -\frac{1}{2\pi}\log\frac{v-u}{v-\bar{u}}$, from which we get

$$d\tilde{G}(u,v) = \frac{1}{2\pi}\left(\frac{du}{v-u} - \frac{d\bar{u}}{v-\bar{u}}\right).$$

As a consequence $F_+(u,v) = \frac{2}{\pi(v-u)}$ and $F_-(u,v) = -\frac{2}{\pi(v-\bar{u})}$.

It is easier to work with the functions $F_\pm = F_0 \pm F_1$ since they transform nicely. Recall that $\tilde{G}$ is conformally invariant, that is if $\phi : V \to U$ is a conformal homeomorphism then $\tilde{G}_V(u,v) = \tilde{G}_U(\phi(u), \phi(v))$. As a consequence $F_\pm$ are conformally covariant:

$$F_+^V(u,v) = F_+^U(\phi(u), \phi(v))\phi'(v).$$

$$F_-^V(u,v) = F_-^U(\phi(u), \phi(v))\overline{\phi'(v)}.$$

This allows us to compute asymptotics of K^{-1} on any Jordan domain.

More precisely, the result is the following. When w, b are *far apart*, we can use the above asymptotic formulas. When they are close together, the dominant term is controlled by (1) with a deviation of order ϵ given by the function(s) $F_+(u,v) - \frac{2}{\pi(v-u)}$ and $F_-(u,v)$.

4.5 Height moment

Here is a sample computation, the expected value of $h(p)h(q)$ in the upper half plane.

Let a_i, b_i be the horizontal edges on a vertical path from p to the x-axis, the a_i being those with a white left vertex, and similarly let c_i, d_i be those for q, see Figure 10.

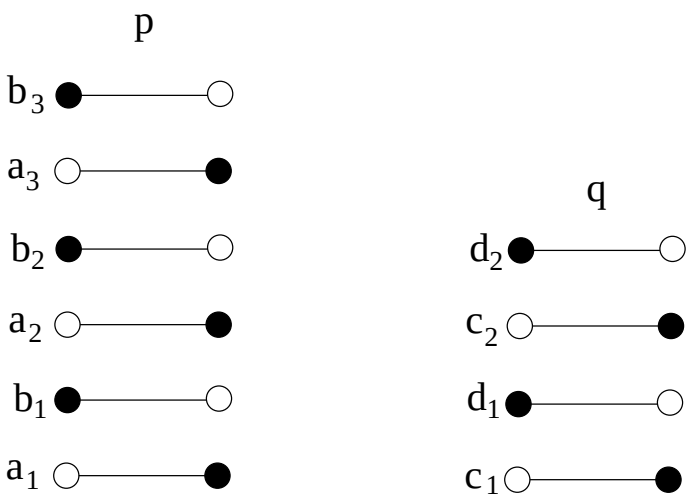

Figure 10:

We have $h(p) = 4\sum_i a_i - b_i$, $h(q) = 4\sum_j c_j - d_j$. So

$$\mathbb{E}(h(p)h(q)) = 16\sum_{i,j} \mathbb{E}(a_i c_j) - \mathbb{E}(b_i c_j) - \mathbb{E}(a_i d_j) + \mathbb{E}(b_i d_j).$$

Each of these terms can be written as the determinant of a 2×2 matrix with

entries in K^{-1}. For example

$$\mathbb{E}(a_i\, c_j) = \det \begin{pmatrix} K^{-1}(a_i^{(0)}, a_i^{(1)}) & K^{-1}(c_j^{(0)}, a_i^{(1)}) \\ K^{-1}(a_i^{(0)}, c_j^{(1)}) & K^{-1}(c_j^{(0)}, c_j^{(1)}) \end{pmatrix}$$

where $a_i^{(0)}, a_i^{(1)}$ are the white and black vertices of a_i, and likewise for c_j. The diagonal terms will all cancel out, and after a certain amount of rearranging, one finds in the limit

$$\begin{aligned} \mathbb{E}((h(p) - \overline{h(p)})(h(q) - \overline{h(q)})) \;=\; & \int_{\gamma_1,\gamma_2} \begin{vmatrix} 0 & F_+(z_1,z_2) \\ F_+(z_2,z_1) & 0 \end{vmatrix} dz_1 dz_2 \\ & - \int_{\gamma_1,\gamma_2} \begin{vmatrix} 0 & F_-(z_1,z_2) \\ \overline{F_-(z_2,z_1)} & 0 \end{vmatrix} d\overline{z_1} dz_2 \\ & - \int_{\gamma_1,\gamma_2} \begin{vmatrix} 0 & \overline{F_-(z_1,z_2)} \\ F_-(z_2,z_1) & 0 \end{vmatrix} dz_1 d\overline{z_2} \\ & + \int_{\gamma_1,\gamma_2} \begin{vmatrix} 0 & \overline{F_+(z_1,z_2)} \\ \overline{F_+(z_2,z_1)} & 0 \end{vmatrix} d\overline{z_1} d\overline{z_2}. \end{aligned}$$

For the upper half-plane we have $F_+(z_1,z_2) = \frac{2}{\pi(z_2-z_1)}$ and $F_-(z_1,z_2) = -\frac{2}{\pi(z_2-\overline{z_1})}$. Plugging these in gives

$$\begin{aligned} & -\frac{4}{\pi^2}\int_{\gamma_1}\int_{\gamma_2} \frac{1}{(z_2-z_1)^2} dz_1 dz_2 + \frac{4}{\pi^2}\int_{\gamma_1}\int_{\gamma_2} \frac{1}{(z_2-\overline{z_1})^2} d\overline{z_1} dz_2 + \\ & \qquad + \frac{4}{\pi^2}\int_{\gamma_1}\int_{\gamma_2} \frac{1}{(\overline{z_2}-z_1)^2} dz_1 d\overline{z_2} - \frac{4}{\pi^2}\int_{\gamma_1}\int_{\gamma_2} \frac{1}{(\overline{z_2}-\overline{z_1})^2} d\overline{z_1} d\overline{z_2}. \end{aligned}$$

The first of these integrals gives

$$-\frac{4}{\pi^2}\log\frac{(p-q)(r-s)}{(p-s)(r-q)}.$$

Therefore

$$\begin{aligned} \mathbb{E}((h(p) - \bar{h}(p))(h(q) - \bar{h}(q))) \;&=\; \frac{4}{\pi^2}\left(-2\mathrm{Re}\log\frac{(p-q)(r-s)}{(p-s)(r-q)} + \right. \\ &\qquad \left. + 2\mathrm{Re}\log\frac{(\overline{p}-q)(r-s)}{(\overline{p}-s)(r-q)}\right) \\ &=\; \frac{8}{\pi^2}\mathrm{Re}\log\left(\frac{\overline{p}-q}{p-q}\right). \end{aligned}$$

Note that this quantity is a multiple of the Dirichlet Green's function $G(p,q)$.

4.6 The Gaussian free field

Let $h_0(p) = h(p) - \overline{h(p)}$ be the fluctuation of h away from the mean. More generally one finds that all the moments of the height fluctuations can be written in terms of Green's functions:

Theorem 4 *Let U be a Jordan domain with smooth boundary. Let $p_1, \ldots, p_k \in U$ be distinct points. If k is odd we have $\lim_{\epsilon\to 0} \mathbb{E}(h_0(p_1)\cdots h_0(p_k)) = 0$. If k is even we have*

$$\lim_{\epsilon\to 0} \mathbb{E}(h_0(p_1)\cdots h_0(p_k)) = \left(-\frac{16}{\pi}\right)^{k/2} \sum_{pairings\ \sigma} G(p_{\sigma(1)}, p_{\sigma(2)})\cdots G(p_{\sigma(k-1)}, p_{\sigma(k)}).$$

By Wick's theorem, this implies that $h_0(x)$ is the unique Gaussian process with covariance function $\mathbb{E}(h_0(x)h_0(y)) = G(x,y)$. This can be taken as a definition of the **massless Gaussian free field**.

An alternate description is as follows.

On U let $\{e_i\}$ be an orthonormal eigenbasis of the Laplacian with Dirichlet boundary conditions, and $\Delta e_i = \lambda_i e_i$.

Define

$$\mathrm{GFF}(x) = \sum_{i=1}^{\infty} \frac{c_i}{\sqrt{|\lambda_i|}} e_i(x)$$

where c_i are independent Gaussians of mean 0 and variance 1.

This series defines a distribution, not a function: the series diverges almost surely almost everywhere. However for a smooth function ψ the series

$$\mathrm{GFF}(\psi) \stackrel{def}{=} \sum_{i=1}^{\infty} \frac{c_i}{\sqrt{|\lambda_i|}} \int_U e_i(x)\psi(x)dx$$

converges almost surely.

Theorem 5 ([12]) *As ϵ tends to 0, h_0 tends weakly in distribution to $4/\sqrt{\pi}$ times the massless free field GFF on U in the sense that for any smooth function ψ on U, the random variable $\epsilon^2 \sum_{x\in U_\epsilon} \psi(x)h_0(x)$ tends in distribution to $\frac{4}{\sqrt{\pi}} GFF(\psi)$.*

It is worth pointing out that, although values of h_0 are integral (after adding a non-random smooth function $\overline{h}$), h_0 converges to a continuous object.

There is a lot more that can be said about the distribution of the value of h and h_0 at a point, or the joint punctual distributions. It can be proved that the distribution of h at a point tends, when scaled by $\sqrt{\log \frac{1}{\epsilon}}$, to a Gaussian with variance equal to some universal constant.

5 FK percolation on critical planar graphs

Up to now we have been working on subgraphs of $\mathbb{Z}^2$. For the dimer model on certain other regular graphs, such as the honeycomb graph, similar results can be obtained. However for more general periodic planar graphs, the situation can be more complicated. In this section we discuss a different but related model, the FK-percolation model, on an interesting family of planar graphs the "isoradial" graphs. For this family of graphs we have a surprising property of the partition function and measures that they depend only on the local structure of the graph, not its long-range order.

In the subsequent section we return to dimers but again on this same family of isoradial graphs.

In this section we will show that the partition function of the random cluster model has a particular form for this special family of planar graphs (which includes the case $\mathbb{Z}^2$).

Recall the definition of the FK-percolation (random cluster) model. Let G be a graph. The space of configurations is $X = \{w : E \to \{0,1\}\}$ (each edge is open or closed).

Let $\nu : E \to (1, \infty)$ be an assignment of weights to the edges, and $q > 0$ a constant.

We define a probability measure on X,

$$\mu(w) = \frac{1}{Z} q^c \prod_{e \text{ open}} \nu(e),$$

where c is the number of connected componets of open edges of w, the product is over open edges of w, and Z is a normalizing constant, called the partition function:

$$Z = \sum_{w \in X} q^c \prod_{e \text{ open}} \nu(e).$$

Note that when $q = 1$ we are reduced to the standard peroclation model. More generally when q is an integer the model is equivalent to the q-state

Potts model [1]; in an appropriate limit $q \to 0$ the model is equivalent to the spanning tree model.

For further information on the model see [7].

5.1 Duality

If G is planar let G^* be its planar dual. Let ν^* be weights on edges e^* of G^*, defined by $\nu^*(e^*) = q/\nu(e)$.

Lemma 4 *For any configuration of edges of G with c components, k edges and r cycles, we have $c - r + k = V$, where V is the number of vertices of G.*

Then we have the following identity between Z and Z^*, the dual partition function:

Proposition 1

$$Z^* = Z \cdot q^{E-V}/W,$$

where W is the product of all of the edge weights $W = \prod_{e \in E} \nu(e)$.

Proof: Suppose A is a configuration of open edges, with c components and weight $q^c \prod_{e \in A} \nu(e)$. The dual configuration has edges $E - A$ and c' components. Its weight is

$$q^{c'} \prod_{e \in E-A} \nu^*(e^*) = q^{c'} \prod_{e \in E-A} \frac{q}{\nu(e)} = q^{c'} \frac{q^{E-A}}{W} \prod_{e \in A} \nu(e),$$

where W is the product of all edge weights of G. But by the Lemma, $c + A - c' = V$, so the weight of a dual configuration is a constant q^{E-V}/W times the weight of the primal configuration. □

In particular the duality is an **isomorphism** between the corresponding probability spaces. As a consequence we have $p_e + p_{e^*} = 1$, where p_e, p_{e^*} are the edge probabilities.

5.2 $Y - \Delta$ transformation

We can sometimes transform G while preserving the measure μ. See Figure 11.

Given a triangle in G with vertices v_1, v_2, v_3 and edge weights $e_{23} = a, e_{13} = b, e_{12} = c$, and a '$Y$' with the same vertices and edge weights A, B, C, (as in Figure 11) we have

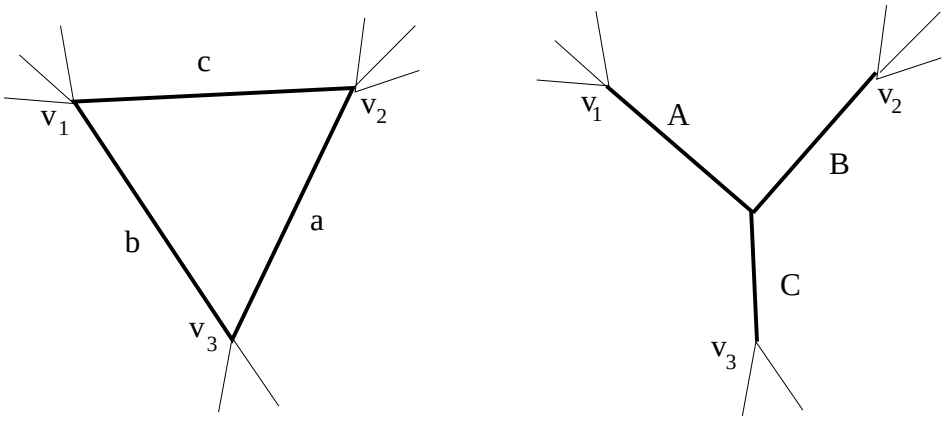

Figure 11:

event	weight in Δ	weight in Y
v_1, v_2, v_3 connected	$(1+a)(1+b)(1+c)$	$q + A + B + C + AB + BC + AC + ABC$
v_1, v_2 connected	$(1+c)(1+\frac{a+b+ab}{q})$	$q + A + B + C + AB + \frac{AC+BC+ABC}{q}$
v_1, v_3 connected	$(1+b)(1+\frac{a+c+ac}{q})$	$q + A + B + C + AC + \frac{AB+BC+ABC}{q}$
v_2, v_3 connected	$(1+a)(1+\frac{b+c+bc}{q})$	$q + A + B + C + BC + \frac{AB+AC+ABC}{q}$
none connected	$1 + \frac{a+b+c}{q} + \frac{ab+ac+bc+abc}{q^2}$	$q + A + B + C + \frac{AB+AC+BC}{q} + \frac{ABC}{q^2}$

Here the events on the left refer to connections via open edges *outside* the triangle. The central column gives the additional (multiplicative) weight due to the possible open edges inside the triangle. The left column gives the additional (multiplicative) weight due to the possible open edges inside the Y.

The $Y - \Delta$ transformation preserves the measures on condition that the weights in the 'Δ' column be proportional to the weights in the 'Y' column. This gives 4 polynomial equations for the weights a, b, c, A, B, C.

Lemma 5 *These equations have a solution only if*

$$-q + ab + ac + bc + abc = 0 \tag{1}$$

and

$$-q^2 - q(A + B + C) + ABC = 0. \tag{2}$$

In this case the solution is

$$A = \frac{q}{a}, \qquad B = \frac{q}{b} \qquad C = \frac{q}{c}. \tag{3}$$

For certain types of graphs/weights, these transformations take on a particularly nice form:

5.3 Isoradial embeddings

This notion is due to Duffin [5] and Mercat [16]. We say G has an **isoradial embedding** if G is drawn so that each face is a cyclic polygon, that is, is inscribable in a circle, and all the circles have radius 1.

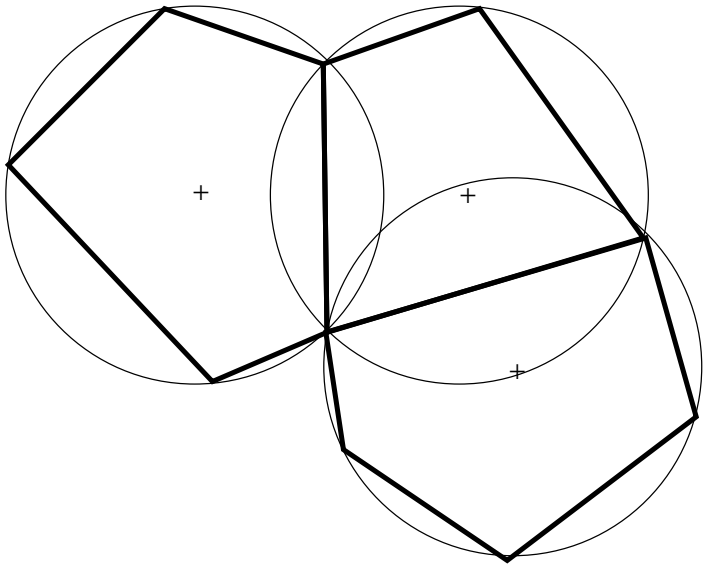

Figure 12: Isoradial embedding of a graph

In this case we can embed G^* isoradially as well, using the circle centers (at least as long as the circle centers are in the interior of the corresponding faces of G). Each edge has a rhombus around it whose vertices are the vertices of the edge and its dual (Figure 13).

Let θ be the half-angle of the rhombus and define

$$\nu(e) = \sqrt{q}\frac{\sin(\frac{2r}{\pi}\theta)}{\sin(\frac{2r}{\pi}(\frac{\pi}{2}-\theta))}$$

where $r = \cos^{-1}(\sqrt{q}/2)$.

Then one may check that

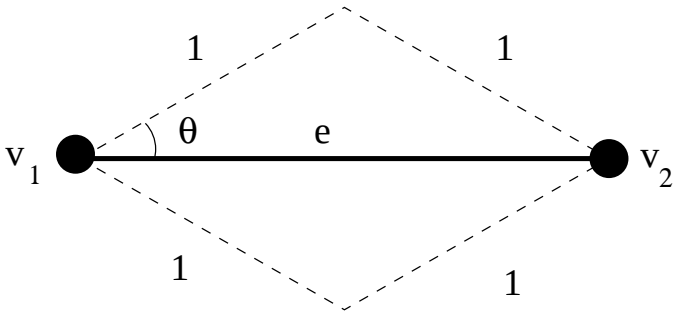

Figure 13:

Lemma 6 *A $Y-\Delta$ transformation preserves isoradiality under these weights.*

This follows from plugging in the weights $\nu(e)$ into (1), and using the fact that a triangle exists only when $\theta_a + \theta_b + \theta_c = \pi/2$.

5.4 Periodic graphs

A planar graph G is **periodic** if translations in $\mathbb{Z}^2$ are (weight-preserving) isomorphisms. In this case $G_n = G/n\mathbb{Z}^2$ is a toroidal graph. Let Z_n be the partition function on G_n. we define $Z = \lim_{n\to\infty} Z_n^{1/|G_n|}$. This is the **partition function per site** for the infinite periodic graph G.

5.5 Main theorem

Here is the main result of this section:

Theorem 6 *There exists a function $F_q : [0, \frac{\pi}{2}] \to \mathbb{R}$ such that for any periodic, isoradial planar graph G, with edge weights ν as above, the partition*

function per site is

$$\log Z = -\frac{1}{2}\log q + \frac{1}{|G_1|}\sum_{\text{edges in a f.d.}} F_q(\theta).$$

The proof doesn't tell us anything about the function F_q. However F_q was computed (non-rigorously) by Baxter [1] (for the graph $\mathbb{Z}^2$, and hence for any isoradial graph). For $q \in (0,4)$ the answer is

$$F_q(\theta) = -\frac{1}{2}\int_{-\infty}^{\infty} \frac{\sinh((\pi - r)t)\sinh(\frac{4r}{\pi}\theta t)}{t\sinh(\pi t)\cosh(rt)}dt.$$

Any information about this integral would be greatly appreciated.

Proof sketch: Each $Y \leftrightarrow \Delta$ changes the partition function by

$$Z_Y = Z_\Delta \frac{q^2}{abc}.$$

Define a new-fangled "partition function"

$$\tilde{Z} = \frac{Zq^{V/2}}{\sqrt{\prod_E \nu(e)}}.$$

It is easy to check that $\tilde{Z}_Y = \tilde{Z}_\Delta$.

The idea is to use $Y - \Delta$ transformations to turn the graph into a graph with large blocks which are copies of big pieces of $\mathbb{Z}^2$. Because G is periodic, each bi-infinite rhombus chain is parallel to copies of itself. We'll rearrange the graph so as to move these chains adjacent to each other in clumps, so that the resulting rhombus tiling consists of large rhombi each tiled with N^2 copies of smaller versions of themselves (Figure 15).

How do we do this transformation? Convert rhombus chains into strings as in Figure 14

Slide the strings around without creating new intersections. When a string crosses the intersection of another pair of strings, the crossing corresponds to a $Y - \Delta$ transformation on the underlying graph. We can slide the strings around until the graph looks like a union of blocks, each tiled by parallel rhombi, as in Figure 15. That is, we can do this unless some rhombus chain is separated from its translates by a third chain which does not intersect either but whose rhombi have a different common parallel. In this case it is possible to show that simply exchanging the chains does not

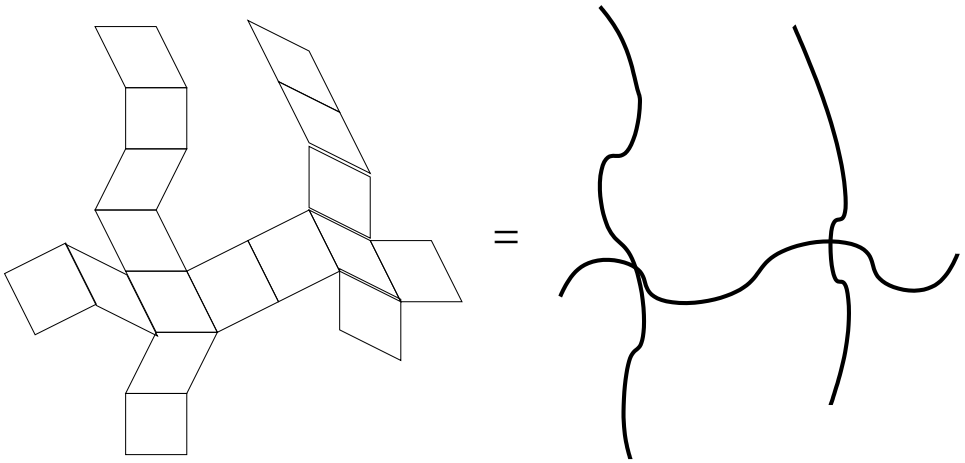

Figure 14:

change the partition function. (One way to see this is to add an extra edge and it's "negative" at the same place so that you can exchange the two rows using a sequence of $Y - \Delta$ moves...)

Now by subadditivity, when there are only large blocks, the partition function can be computed separately on each block and the results multiplied together (with an error of lower order). But on each block the graph is a piece of $\mathbb{Z}^2$ and the partition function is $\exp(Ac(1 + o(1)))$ where A is the area and c a function of the angle only. Letting $N \to \infty$ we can conclude in that $\tilde{Z} = \prod_{edges} F_q(\theta)$ for some F_q. The result follows. □

This theorem has some nontrivial consquences even without knowing F_q. For example let Z_{rect} be the partition function per site for the graph $\mathbb{Z}^2$ with edge lengths 1 vertically and $\sqrt{3}$ horizontally (and corresponding weights ν as above). Let Z_{hex} be the partition function per site for the honeycomb graph with edge lengths 1. Then

$$\frac{Z_{\text{rect}}}{Z_{\text{hex}}} = \frac{2\cos(\frac{2}{3}\cos^{-1}(\frac{\sqrt{q}}{2}))}{q^{1/6}}.$$

As another "application" of the theory, it is natural to conjecture that the FK-percolation model is critical for weights ν. For example in standard percolation ($q = 1$) we should have $p_c/(1 - p_c) = \nu$.

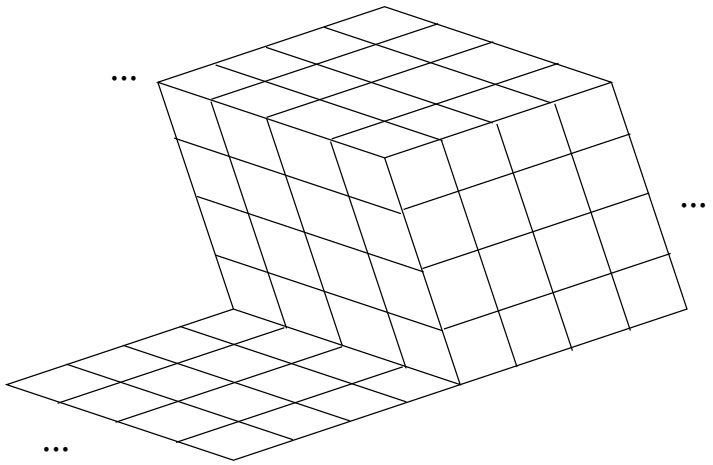

Figure 15:

For example on the on the honeycomb lattice the critical probability should be

$$p_c = \frac{2\cos\frac{\pi}{9}}{1+2\cos\frac{\pi}{9}} \approx 0.652704.$$

This was in fact proved for the honeycomb lattice by Wierman [19].

Proposition 2 *The only function f for which $(a,b,c) = (f(\theta_a), f(\theta_b), f(\theta_c))$ satisfies (1) when $\theta_a + \theta_b + \theta_c = \pi/2$ and (3) is*

$$f(\theta) = \sqrt{q}\frac{\sin\left(\frac{2r}{\pi}\theta\right)}{\sin\left(\frac{2r}{\pi}(\frac{\pi}{2}-\theta)\right)}$$

where $r = \cos^{-1}(\sqrt{q}/2)$.

6 Integrability and dimers on critical planar graphs

Surprisingly, the same isoradiality condition which worked so well in the random cluster model also has a simplifying effect on the dimer partition function.

Let G be a bipartite planar graph. We embed G isoradially. Let $\nu(e) = \sin 2\theta$, where θ is the half-angle of the corresponding rhombus. We use these weights to define a probability measure on perfect matchings of (finite subgraphs of) G as we did before: the probability of a matching is proportional to the product of its edge weights.

We define a Kasteleyn matrix as follows: if $e = wb$ is an edge with dual edge $e^* = p^*q^*$, then $K(w, b) = i(p^* - q^*)$.

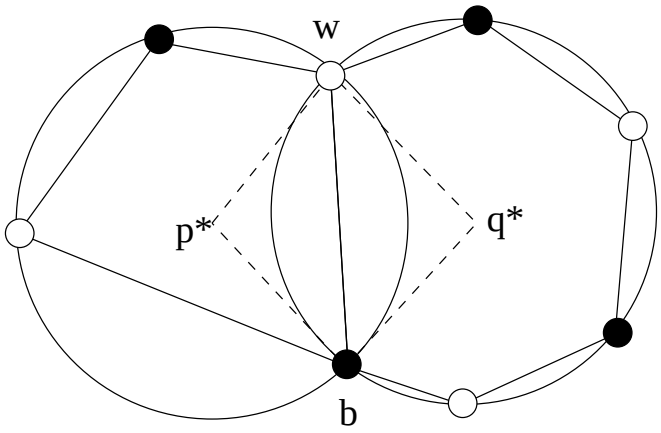

Figure 16:

Lemma 7 *K is a Kasteleyn matrix for (any finite simply connected subpiece of) G.*

Note that $|K(w, b)| = 2 \sin \theta$.

Proof: It suffices to show that K is Kasteleyn-flat [15], that is, we must show that for each face of G_1 with vertices $u_1, v_1, \ldots, u_m, v_m$ in cyclic order, we have

$$\arg(K(u_1, v_1) \ldots K(u_m, v_m)) = \arg((-1)^{m-1} K(v_1, u_2) \ldots K(v_{m-1}, u_m) K(v_m, u_1)).$$

(This identity implies that two dimer configurations which only differ around a single face have the same argument in the expansion of the determinant.

By [15], any two configurations can be obtained from one another by such displacements.) To prove this identity, note that it is true if the points are regularly spaced along a $2m$-gon, and note that it remains true if you move one point at a time. □

There are two main results in this section, an explicit computation of Z and K^{-1}.

Theorem 7 *The determinant per site of K satisfies*

$$\log Z = \frac{1}{N} \sum_{edges\ e} \frac{1}{\pi} L(\theta) + \frac{\theta}{\pi} \log 2 \sin \theta,$$

where $\nu(e) = 2\sin(\theta(e))$, N is the number of vertices in a fundamental domain, the sum is over the edges in a fundamental domain, and L is the Lobachevsky function,

$$L(x) = -\int_0^x \log 2 \sin t dt.$$

To describe K^{-1}, first define for any complex parameter z an **elementary discrete analytic function** to be a function satisfying $f_{v'} = f_v/(z - e^{i\alpha})$, if vv' leads away from a white, or towards a black vertex, and $f_{v'} = f_v \cdot (z - e^{i\alpha})$, if vv' leads away from a black, or towards a white vertex. Such an f is well-defined the product of the multipliers going around a rhombus leads back to the starting value.

Theorem 8 *We have*

$$K^{-1}(b, w_0) = -\frac{1}{2\pi i} \sum_{poles\ e^{i\theta}} \theta \cdot Res_{z=e^{i\theta}}(f_b/f_{w_0}), \tag{1}$$

where the angles $\theta \in \mathbb{R}$ are chosen appropriately. This can be written

$$\frac{1}{4\pi^2 i} \int_C \frac{f_b(z)}{f_{w_0}(z)} \log z dz,$$

where C is a closed contour surrounding cclw the part of the circle $\{e^{i\theta} \mid \theta \in [\theta_0 - \pi + \epsilon, \theta_0 + \pi - \epsilon]\}$ which contains all the poles of f_b, and with the origin in its exterior.

Proof: Let $F(b)$ denote the right-hand side of (1). We will show that $\sum_{b\in B} K(w,b)F(b) = \delta_{w_0}(w)$, and $F(b)$ tends to zero when $b \to \infty$.

Let C_θ be a small loop around $e^{i\theta}$ in $\mathbb{C}$. We have

$$\begin{aligned}
\sum_{b\in B} K(w,b)F(b) &= \sum_{j=1}^{k} i(-e^{i\theta_j} + e^{i\theta_{j-1}})F(b_j), \\
&= -\frac{1}{2\pi i}\sum_{j=1}^{k} i(-e^{i\theta_j} + e^{i\theta_{j-1}}) \sum_{\text{poles } e^{i\theta}} \theta \cdot \mathrm{Res}_{z=e^{i\theta}}(f_{b_j}) \\
&= -\frac{1}{2\pi} \sum_{\text{poles } e^{i\theta}} \theta \cdot \sum_{j=1}^{k}(-e^{i\theta_j} + e^{i\theta_{j-1}})\frac{1}{2\pi i}\int_{C_\theta} f_{b_j}(z)dz \\
&= -\frac{1}{2\pi} \sum_{\text{poles } e^{i\theta}} \frac{\theta}{2\pi i}\int_{C_\theta} f_w(z) \sum_{j=1}^{k} \frac{(-e^{i\theta_j} + e^{i\theta_{j-1}})}{(z - e^{i\theta_j})(z - e^{i\theta_{j-1}})}dz \\
&= -\frac{1}{2\pi} \sum_{\text{poles } e^{i\theta}} \frac{\theta}{2\pi i}\int_{C_\theta} f_w(z) \left(\sum_{j=1}^{k} \frac{1}{(z - e^{i\theta_{j-1}})} - \frac{1}{(z - e^{i\theta_j})}\right) dz \\
&= -\frac{1}{2\pi} \sum_{\text{poles } e^{i\theta}} \frac{\theta}{2\pi i}\int_{C_\theta} 0dz = 0.
\end{aligned}$$

However when $w = w_0$ we have

$$F(b_j) = -\frac{1}{2\pi i}\left(\frac{\theta_j - \theta_{j-1}}{e^{i\theta_j} - e^{i\theta_{j-1}}}\right),$$

so that

$$\sum_{j=1}^{k} i(-e^{i\theta_j} + e^{i\theta_{j-1}})F(b_j) = \frac{1}{2\pi}\sum_{j=1}^{k} \theta_j - \theta_{j-1} = 1,$$

since the angles increase by 2π around w_0.

To complete the proof, one must show that $F(b) \to 0$ as $b \to \infty$. □

Proposition 3 *We have*

$$K^{-1}(b,w) = \frac{1}{2\pi}\left(\frac{1}{b-w} + \frac{\gamma}{(\bar{b} - \bar{w})}\right) + O\left(\frac{1}{|b-w|^2}\right),$$

where $\gamma = f_b(0) = e^{-i(\theta_1+\theta_2)}\prod e^{i(-\beta_j+\alpha_j)}$, *and the angles are as illustrated in Figure 17.*

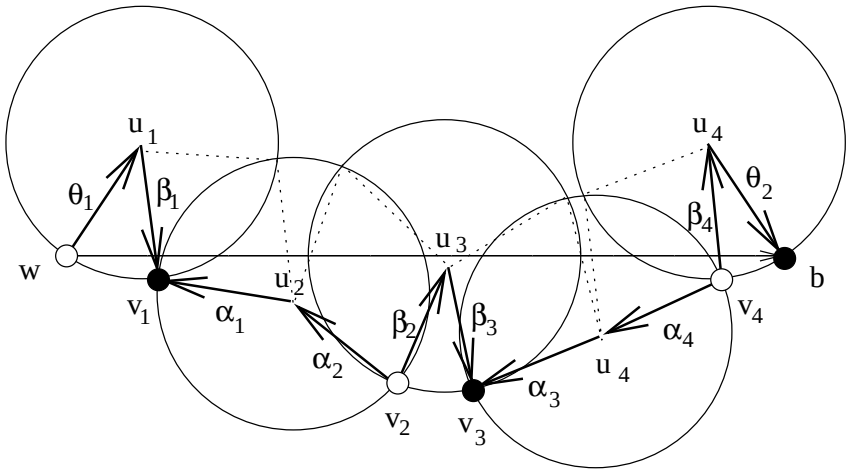

Figure 17:

6.1 Determinants

For a finite graph G we define the **normalized determinant**, or determinant **per site**, $\det_1 M$ of an operator $M\colon \mathbb{C}^G \to \mathbb{C}^G$ to be

$$\det_1 M \stackrel{\text{def}}{=} |\det M|^{1/|G|},$$

where $|G|$ is the number of vertices of G.

For an operator M on a finite graph, $\det M$ is a function of the matrix entries $M(i,j)$ which is linear in each entry separately. In particular for an edge $e = ij$, as a function of the matrix entry $M(i,j)$ we have $\det M = \alpha + \beta M(i,j)$, where β is $(-1)^{i+j}$ times the determinant of the minor obtained by removing row i and column j. That is,

$$\frac{\partial(\det M)}{\partial(M(i,j))} = M^{-1}(j,i) \cdot \det M,$$

or

$$\frac{\partial(\log\det M)}{\partial M(i,j)} = M^{-1}(j,i). \tag{2}$$

Suppose that G is periodic under translates by a lattice Λ. Let $G_n = G/n\Lambda$, the finite graph which is the quotient of G by $n\Lambda$. Now if we sum (2) for all Λ-translates of edge ij in G_n, and then divide both sides by $|G_n|$, it yields

$$\frac{\partial(\log \det_1 M)}{\partial M(i,j)} = \frac{1}{|G_1|} M^{-1}(j,i), \tag{3}$$

where $M(i,j)$ is now the common weight of all translates of edge ij, that is, the left-hand side is the change in $\log \det_1 M$ when the weight of all translates of ij changes. Note that this equation is independent of n.

It is now a short computation to compute the determinant of K from the exact form of K^{-1}....see [13]

6.2 Isoradial embeddings

The set of isoradial embeddings $\mathrm{ISO}(G)$, when parametrised by the rhombus angles, is convex. This follows because an isoradial embedding is determined from a set of rhombus angles by the linear conditions that the sum around each vertex must be π.

There is a unique (possibly degenerate) isoradial embedding maximizing Z, because Z is strictly concave on $\mathrm{ISO}(G)$.

(Joint with J-M. Schlenker) A **zig-zag** path in a planar graph is a path which turns maximally left at a vertex, then maximally right at the next vertex, then maximally left, and so on. That is, it leaves from a vertex along an edge which is adjacent in cyclic order to the edge it entered on, alteranting to the right and to the left. A planar graph has an isoradial embedding if and only if the following two conditions are satisfied (Figure 18):

1. No zig-zag path crosses itself
2. No two zig-zag paths cross more than once.

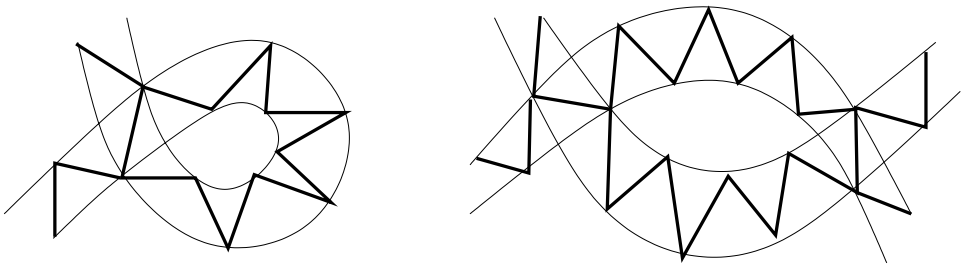

Figure 18: Not allowed in isoradial graphs

It is not hard to see why these conditions are necessary: a zig-zag path corresponds to a rhombus chain in an isoradial embedding, and such a chain is monotone and so cannot cross itself. Two such chains cannot cross more than once due to the orientation of their common rhombi.

6.3 Hyperbolic ideal polyhedra

To an isoradially embedded graph G we can associate an ideal polyhedron in $\mathbb{H}^3$ as follows. Suppose G is embedded on the xy plane which is the boundary at ∞ of the upper half-space model of $\mathbb{H}^3$. Vertices of P are vertices of G^* (circle centers) and edges of P are geodesics which project vertically to the edges of G^*.

The volume of P per fundamental domain can be seen to be the same as the entropy per fundamental domain of the dimer model on G. That is,

$$\frac{1}{\pi}\mathrm{Vol}(P) = \frac{1}{\pi}\sum_{e\in\text{f.d.}} L(\theta) = \log Z - \sum_{e\in\text{f.d.}} \Pr(e)\log\nu(e).$$

Moreover the term

$$\sum_{e\in\text{f.d.}} \Pr(e)\log\nu(e) = \sum_{e\in\text{f.d.}} \frac{\theta}{\pi}\log 2\sin\theta$$

can be associated with the mean curvature of P, which is by definition the sum over the edges of the dihedral angle times the (normalized) hyperbolic edge length.

Question: Can one construct a tiling in some canonical (entropy-preserving) way using the geodesic flow inside P?

References

[1] R. Baxter, Exactly solved models in statistical mechanics. Academic Press.

[2] R. Burton, R. Pemantle, Local characteristics, entropy and limit theorems for spanning trees and domino tilings via transfer-impedances, *Ann. Prob.* **21**,no. 3(1993) 1329-1371.

[3] H. Cohn, N. Elkies, J. Propp, Local statistics for random domino tilings of the Aztec diamond. *Duke Math. J.***85** (1996), no. 1, 117–166.

[4] H. Cohn, R. Kenyon, J. Propp, A variational principle for domino tilings. *J. Amer. Math. Soc.* **14** (2001), no. 2, 297–346.

[5] R. J. Duffin, Potential theory on a rhombic lattice. *J. Combinatorial Theory***5**(1968) 258–272.

[6] N. Elkies, G. Kuperberg, M. Larsen, J. Propp, Alternating-sign matrices and domino tilings. I. *J. Algebraic Combin.* **1** (1992), no. 2, 111–132.

[7] G. Grimmett, The stochastic random-cluster process and the uniqueness of random-cluster measures. *Ann. Probab.***23** (1995), no. 4, 1461–1510.

[8] P. W. Kasteleyn, The statistics of dimers on a lattice. I. The number of dimer arrangements on a quadratic lattice, *Physica* **27** (1961), 1209–1225.

[9] P. W. Kasteleyn, Graph theory and crystal physics, 1967 Graph Theory and Theoretical Physics pp. 43–110, Academic Press, London

[10] R. Kenyon, Local statistics of lattice dimers, *Ann. Inst. H. Poincaré, Prob. et Stat.* **33** (1997), 591-618.

[11] R. Kenyon, Conformal invariance of domino tiling, *Ann. Prob.* **28** (2000).

[12] R. Kenyon, Dominos and the Gaussian free field, *Ann. Prob.* **29** (2001).

[13] R. Kenyon, The Laplacian and Dirac operators on critical planar graphs, preprint.

[14] R. Kenyon, J. Propp, D. Wilson, Trees and Matchings, *El. J. Combin.* **7** (2000), Research paper 25, 34pp.

[15] G. Kuperberg, An exploration of the permanent-determinant method. *Electron. J. Combin.***5** (1998), no. 1, Research Paper 46, 34 pp. (electronic)

[16] C. Mercat, Discrete Riemann surfaces and the Ising model. *Commun. Math. Phys.* **218**(2001),177-216.

[17] H. Temperley, Combinatorics: Proceedings of the British Combinatorial Conference 1973, *London Math. Soc. Lecture Notes Series #13*, (1974) 202-20

[18] M. Fisher, H. Temperley, The dimer problem in statistical mechanics – an exact result. *Phil Mag.* **6**(1961), 1061-1063.

[19] J. Wierman, Bond percolation on honeycomb and triangular lattices. *Adv. in Appl. Probab.***13** (1981), no. 2, 298–313.